Journal of Mechanical Engineering and Sciences
ISSN (Print): 2289-4659; e-ISSN: 2231-8380
Volume 13, Issue 1, pp. 4449-4460, March 2019

DOI: https://doi.org/10.15282/jmes.13.1.2019.08.0378

Fracture cause analysis of the extruder's shaft and geometry optimization of the spline

O. Lyashuk[1]*, Y. Pyndus[1], I. Lutsiv[2], Y. Vovk[3], L. Poberezhna[4], O. Tretiakov[1] and R. Zolotyy[5]

[1]Department of Automobile Transport, Ternopil Ivan Puluj National Technical University, 56 Rus'ka Street, 46001 Ternopil, Ukraine
Phone: +380352519700; Fax: +380352254983
*Email: oleglashuk@ukr.net
[2]Department of Designing Metal-Cutting Machine and Tools, Ternopil Ivan Puluj National Technical University, 56 Rus'ka street, 46001 Ternopil, Ukraine
[3]Department of Transport Technologies and Mechanics, Ternopil Ivan Puluj National Technical University, 56 Rus'ka Street, 46001 Ternopil, Ukraine
[4]Department of Medical Informatics, Medical and Biological Physics, Ivano-Frankivsk National Medical University, 2 Halytska street, 76018 Ivano-Frankivsk, Ukraine
[5]Department of Automation Technological Processes and Production, Ternopil Ivan Puluj National Technical University, 56 Rus'ka Street, 46001 Ternopil, Ukraine

ABSTRACT

The article is devoted to increasing of the durability of technological equipment elements, forecasting of the resource and diagnostics of failures of the technical system. The basic regularities are analyzed and causes of the failure of the extruder's working body shaft are determined. For torque values M = 40.74 - 64.37 N·m and of the extruder's working body shaft, the stress-strain state of the contact surfaces of the keyhole of the extruder's shaft is calculated by the method of three-dimensional finite element modelling. The maximum values of the stress intensity $\sigma_{int(max)}$, which arise on the edge of the key groove, are calculated. It was established that an increase in the distance of the key groove to the fillet of the working body shaft by 2.0 mm leads to a decrease in the maximum stresses on the edge of the key groove by 15.72%. The results of the research allow optimizing the geometry of the shaft.

Keywords: Shaft; spline; finite element method; working body; equipment; drive.

INTRODUCTION

Increase of manufacturing equipment elements' durability, service life prediction and failure diagnosis of engineering systems are significant scientific and engineering problems [1]. Extensive work has been carried out by failure analysis research community investigating the nature of fatigue failures using analytical, semi-empirical and experimental methods [2]. Some gear shaft failures have been reported and common causes of failure have been high stresses, friction or fretting [3-5]. Such measures are especially important for the extruders,

which operate in the conditions of significant technological loads that cause wear of their operating devices and possibility of fracture of separate components.

Generally, shafts do not have a uniform diameter, and they are stepped with shoulders where bearings, gears, or other components are mounted. In the shaft design analysis, it is important to ensure that the shaft geometry will satisfy the material strength requirements and shaft-supported element requirements. Stress analysis at specific points depends on the local geometry, while slope and deflection analysis relies on the overall dimensions of the shaft [2-6]. Stresses concentrate in shaft shoulders and key ways and depend on the local dimensions [3]. Shafts mostly work under the influence of fluctuated loads or combined torsion and bending loads. If a shaft supports a static load, the bending stresses are fully reversed and the torsion is steady [2, 7].

To determine the failure modes, analytical, experimental, and finite element analysis methods can be used [8]. Failure cause analysis requires complete information about the component geometry, material, load condition, work environment, and work constraints [9, 10]. Generally, shafts suffer from a transverse deflection as a beam and a torsion deflection as a torsion bar [11]. In addition, surface failure is a common failure mode of shafts [12, 13]. Fatigue failure, due to recurrent load or overload, stress concentration, insufficient clearance and wrong bearing arrangement, is also possible to happen [10].

Also known are cases of extruder's operating device shaft fracture, which are caused by defects that initiating during operation and are source of cracks initiation and propagation to the critical size [14-17]. This requires increased attention and additional research for more reliable assessment of the shafts' fatigue life. Linear fracture mechanics approaches were used for strength and durability calculation of the drive shaft [18, 19]. They allow to create design models for engineering analysis of the "shaft – operating device" extruder's units and optimize their parameters [20]. This work refers to the determination of the stress-strain state of the spline contact surfaces of the extruder's shaft by a three-dimensional finite element modelling method.

The purpose of the work is to study the stress-strain state of the spline contact surfaces of the extruder loaded shaft and propose a way to reduce them by changing the design of the extruder shaft.

SERVICE CONDITIONS OF EXTRUDERS AND THEIR LOAD-CARRYING ELEMENTS

Constructions of helical operating devices of extruders can be widely used in the food and processing industries due to advanced technological capabilities at the expense of increased reliability and improved design.

Getting high quality products (forage mixture) is possible for stable extruder's operation in equilibrium mode. However, in practice there are several factors, which affect the performance of the extruder and amount of extruded product. Therefore, most extrusion devices have a coefficient of efficiency 45-75% for a satisfactory extrudate quality.

In this work the extrusion device for preparing a forage mixture is investigated [21, 22] Figure 1(a) and (b) in the form of a frame on which the electric motor with a drive is rigidly fixed at the bottom part and in the upper part of the drive a flywheel with a pulley and operating device shaft are set. On the outer diameter of the shaft, separate conveyor screw

sections are set rigidly with the possibility of axial displacement. On the outer diameter of the screws, 3-4 turns of different steps are threaded (Figure 2, (a)). Moreover, conveyor screws are set closely, in the form of a continuous screw line. The 8 - 12 semicircular through splines with the possibility of relative movement at velocity more than 1000 rpm are made in the inner diameter of the sleeve.

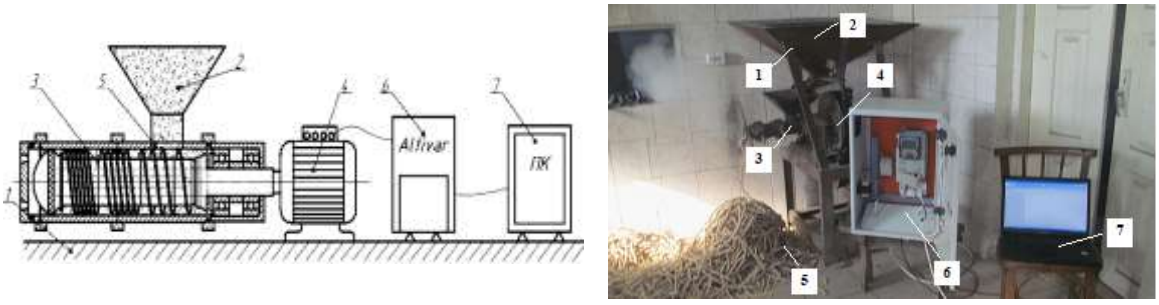

(a) (b)

Figure 1. Construction arrangement for preparing a forage mixture: (a) general view of the experimental screw extruder, (b) 1 – frame, 2 – hopper, 3 – conveyor screw sections, 4 – drive flywheel, 5 – loose material, 6 – Altivar and 7 – computer.

The quality of the finished product is closely interrelated with productivity and depends on design characteristics of extruder operating devices, Figure 2(a) and (b).

(a) (b) (c)

Figure 2. Extruder operating device: (a) shaft, (b) fracture surface of the shaft and (c) crack origin location at A.

SHAFT FRACTURE MECHANISM

By analyzing fracture surface, it was discovered that the crack has a fatigue nature and was initiated from the spline. Hardening and subsequent tempering caused the appearance of thermal microcracks at the bottom of the spline. It should be noted that the crack has a fairly smooth surface that is unusual for cyclic loading with sufficiently large torque. This indicates that failure has taken place due to the achievement of the crack maximum length [23-25, 26-29]. The current level of knowledge about the nature of damage accumulation of long-term exploited constructions allows us to establish several causes of construction failure and to formulate directions of extension of its durability.

Nucleus (short) crack is a consequence of the stress localization and its influence on the construction material. Crack initiation is mainly due to two factors: dislocations accumulation and cleavage of the secondary phases, in particular carbides. Optimization of the element's heat treatment is one of the ways to solve this problem.

Shaft failure in the stress concentration zone is a consequence of the destruction of ties caused by the localization of the deformation process. Therefore, preventing failure is possible providing quantitative analysis of the stress in the vicinity of the concentrator and "unloading" of adjacent areas that requires concentrator geometry optimizations.

RESEARCH METHODOLOGY

One of the most effective modern approaches to stress-strain state assessment of elements of the extruder's operating device Figure 2 (b), (c) is the use of the finite elements method (FEM). The idea of this method is to describe the body under study by some model that represents a set of elements with a finite number of degrees of freedom [14]. When calculating using FEM, solutions of integral and differential equations in partial derivatives are found. FEM is well suited for simulating complex environments and in cases when the desired accuracy (discretization) varies in different parts of the environment.

The stress-strain state of spline contact surfaces of the loaded shaft Figure 3 was calculated in elastic formulation by FEM using the ANSYS software. The material was considered as isotropic. The modulus of elasticity of steel was $E = 2\times10^5$ MPa, Poisson's coefficient $\nu = 0.3$.

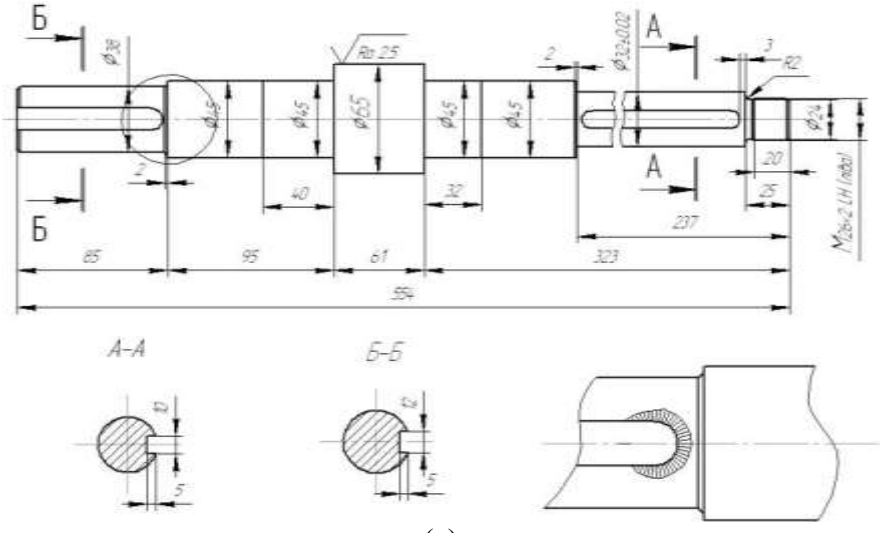

(a)

(b)

Figure 3. (a) Draft of the extruder's operating device shaft and (b) general view of the extruder's operating device shaft.

Three-dimensional solid model of the extruder's shaft with splines was created in the FEM software complex ANSYS APDL and is depicted in Figure 4. The stress-strain state of the contact surfaces of the spline and the key groove of the shaft loaded with torque was investigated Figure 4 (a), (b).

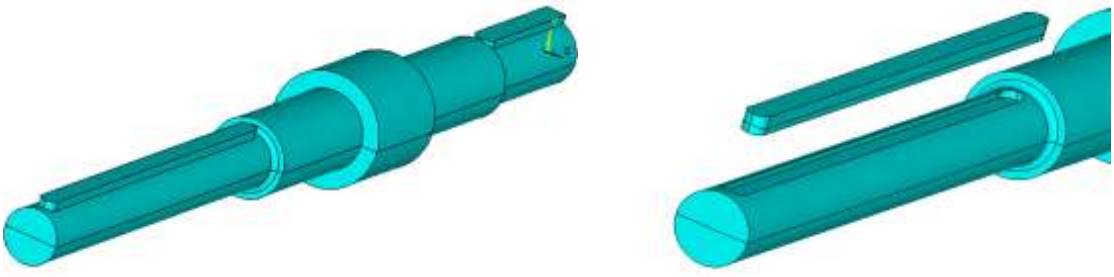

(a) (b)

Figure 4. Solid model of the shaft for stress-strain state investigation of the contact surfaces of the spline and the key groove by FEM: (a) model with matched spline and groove, (b) spaced spline and key groove

Three-dimensional finite element SOLID186 with 20 nodes (including intermediate ones) was used for shaft solid model discretization. This finite element type can transform and acquire the prismatic, pyramidal and tetrahedral forms suitable for modelling of complex solid bodies. The specified element has three degrees of freedom and has properties of elasticity, plasticity, creep, hyper-elasticity. Discretized by finite elements SOLID186 model of the shaft with splines shown in Figure 5 (a). On the contact surfaces of the spline and the key groove finite element mesh was adapted to 0.24 mm size, which is shown in Figure 5 (b).

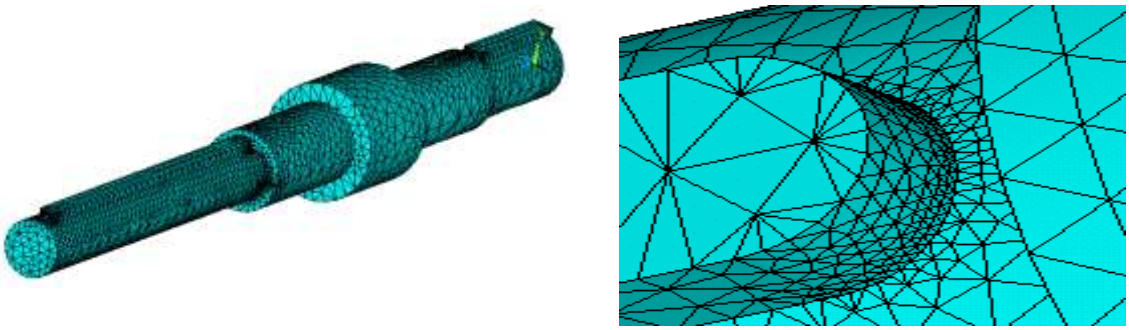

(a) (b)

Figure 5. Finite element model of the shaft: (a) model with matched spline and groove; (b) finite element mesh adaptation on the contact surface of the spline.

Using software tool Contact Manager [15] and finite elements CONTA174 (contact surfaces of the spline) and TARGE170 (contact surfaces of the key groove – contact targets) contact surfaces between spline and key groove were modelled Figure 6. These elements are two-dimensional and they are programmatically imposed on the main SOLID186 elements of the finite element mesh.

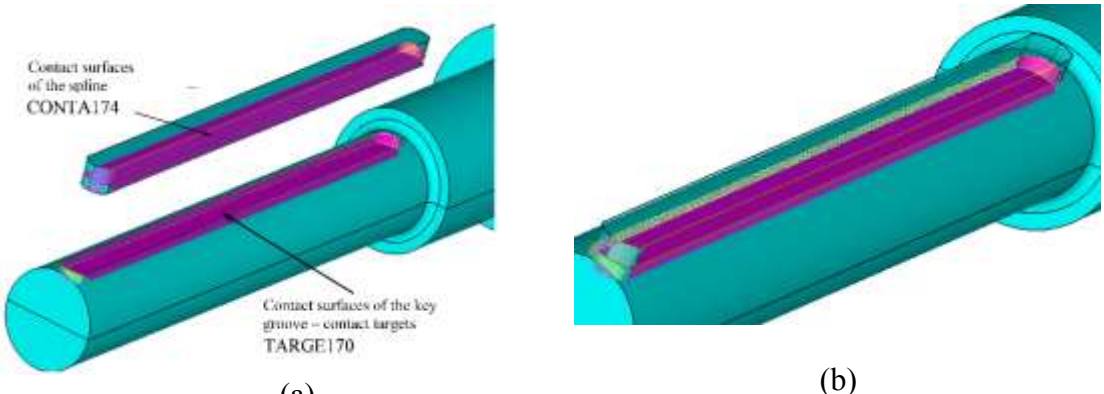

(a) (b)

Figure 6. Spaced (a) and matched (b) contact surfaces of the key groove and the spline.

To create a torque marked side surface Figure 7 of the shorter spline was loaded with normal pressure *P* that is required for a given torque. Marked on the opposite side surface of the spline under study (longer one) was restricted to move along the X axis. To fix model in space the shaft axis was restricted to move along X and Y axes. Point O of the model Figure 7 was restricted to move along X, Y and Z axes.

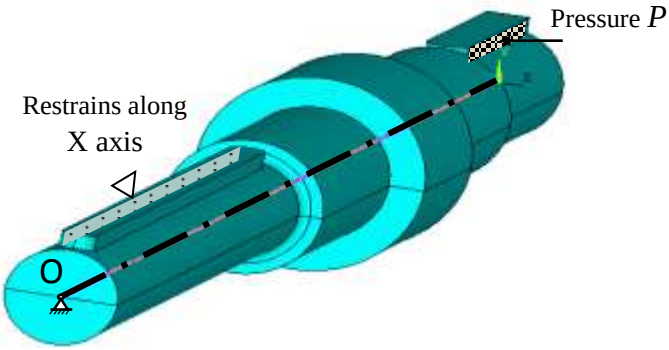

Figure 7. Three-dimensional restrains and loading of the shaft finite element model.

Calculation results of the stress intensity field on the edge of the loaded shaft's spline are shown in Figure 8. Stress intensity was assessed along line *l* showed in Figure 9. To start the motor and adjust the frequency of its rotation the Altivar 71 frequency converter and Power Suite v.2.5.0 software was used. After completing the material extrusion process in the Power Suite window, the computer display received data on the torque change, engine power in time. The torque values are M = 40.742 - 64.372 N·m.

It is found that the rounding radius of the spline causes stress concentration for the fillets of 3.0 and 5.0 mm. It should be taken into account that the reduction of the radius of the concentrator reduces the volume of loaded metal. This is important for the operational conditions of evaluating the technical condition of the construction. It is known that the embrittlement effect of stress concentrators is due not only to the overstress they create in local areas, but also to deformation strengthening as a result of force influence [24, 25, 30-35].

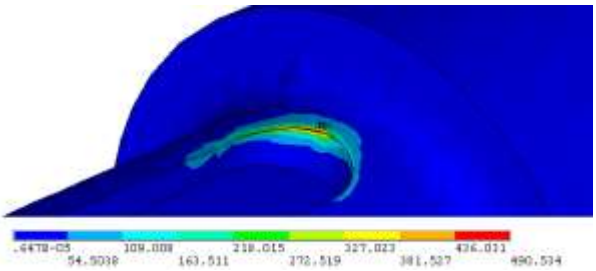

Figure 8. (a) The stress intensity field on the edge of the loaded shaft's spline.

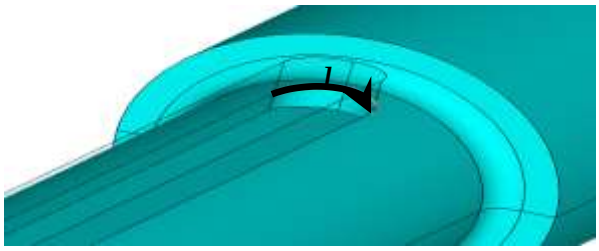

Figure 9. Line *l* along the edge of the spline where maximal operational stress occurs.

RESULTS AND DISCUSSION

The radius of rounding of the keyhole causes the stress concentration at the edge of the shaft groove (Fig. 8) at the crack location. Estimation of the variation of the stresses σint along line l on the edge of the key groove (Fig. 9) with the increase in torque. *Stress intensity* σ_{int} means the largest of the absolute values of principal stresses differences $\sigma_1 - \sigma_2$, $\sigma_2 - \sigma_3$, or $\sigma_3 - \sigma_1$ [20]

$$\sigma_{int} = MAX(|\sigma_1 - \sigma_2|\ |\sigma_2 - \sigma_3|\ |\sigma_3 - \sigma_1|). \quad (1)$$

The calculations were performed for two cases of the geometry of the fillet R = 3.0 mm and R = 5.0 mm (Figure 10).

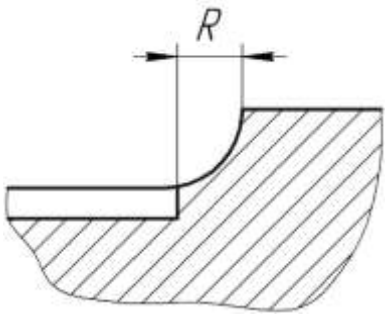

Figure 10. The geometry of the fillet, preceded by the key way groove.

The stress-strain state of the shaft was modelled by FEM. The advantage of using FEM is, first, that it allows you to receive and visualize strains distributions (Figure 8). The curves for stress intensity distribution σ_{int} along the line *l* according to torque are given below (Fig. 11). It is obvious that increasing the distance *R* to the keyhole leads to a decrease in the stresses on the edge of the key groove (Fig. 11).

The maximal values of the intensity of the stress $\sigma_{int(max)}$ on the edge of the key groove after the increase in torque and the influence of the distance *R* of the pin-groove to the fillet are taken into account (Fig. 12). Increasing the distance *R* from the fillet to the key groove from 3.0 mm to 5.0 mm leads to a decrease in the maximum stresses on the edge of the key groove by 15.72%. The established regularities allow optimizing the geometry of the shaft in terms of ensuring its bearing capacity.

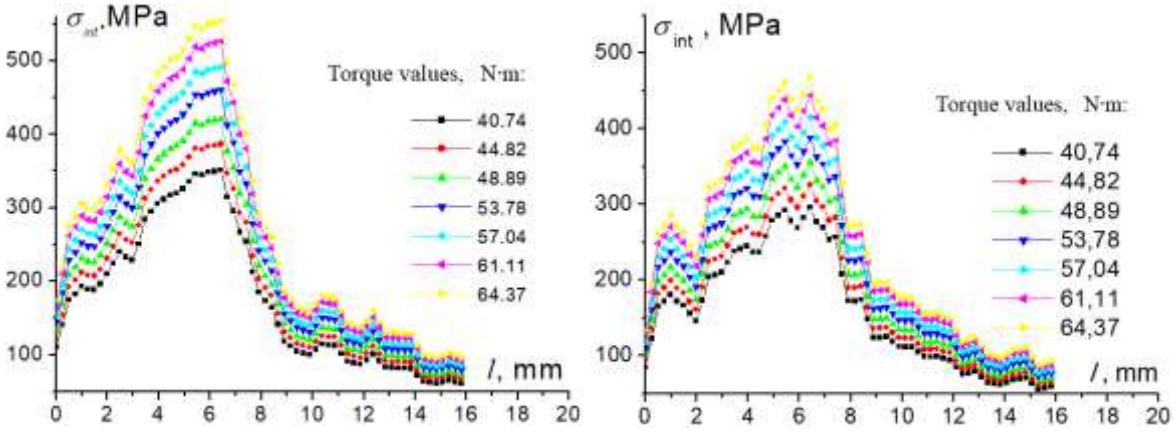

(a) (b)

Figure 11. Stress intensity distribution σ_{int} along line l with increasing torque: (a) fillet 3 mm and (b) fillet 5 mm.

It should be noted that the decrease in the intensity of stress $\sigma_{int(max)}$ can indirectly indicate an increase in cyclic durability of this shaft, which will be caused by a decrease in the maximum values of cyclic deformations in the stress concentration zone [36].

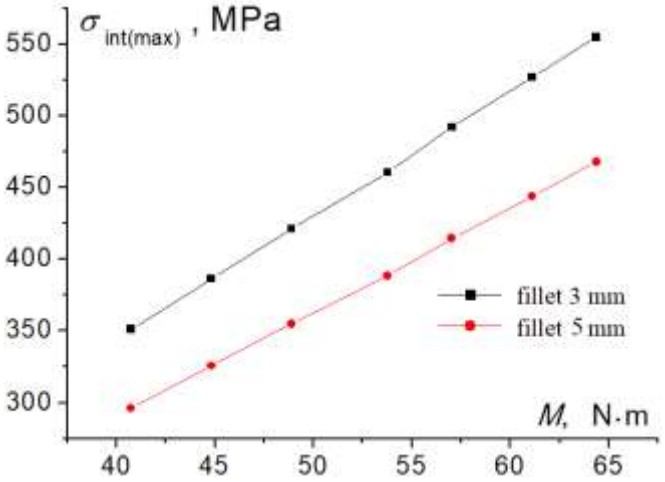

Figure 12. Maximum stress intensity values $\sigma_{int(max)}$ that occur on the edge of the spline with increasing shaft's torque and taking into account the distance from the spline to the fillet.

CONCLUSIONS

Main regularities were analyzed and causes of the failure of the extruder's operating device shaft were determined. It allowed to provide a finite element modelling of its loading and to assess the influence of drive torque on the stress concentration in the spline of the shaft. Increase of torque of the extruder's operating device shaft causes a linear increase in the stress intensity maximum value $\sigma_{int(max)}$ on the edge of the spline. Increasing the distance R from the fillet to the spline by 2 mm leads to a decrease in the maximum stress on the edge of the spline by 15.72%. In perspective, it's worth assessing the period of the fatigue crack nucleation in the place of maximum stress using the S-N diagram.

REFERENCES

[1] Cicero S, Cicero R, Lacalle R, Diaz G, Ferreño D. Failure analysis of a lift gear shaft: Application of the FITNET FFS procedure fatigue module. Engineering Failure Analysis 2008;15:970-980.
[2] Rice RC. Fatigue design handbook. 3rd ed. York: SAE; 1997.
[3] Xu X, Yu Z, Ding H. Failure analysis of a diesel engine gear shaft. Eng Fail Anal 2006;13(8):1351-7.
[4] Sorochak A, Maruschak P, Prentkovskis O Cyclic fracture toughness of railway axle and mechanisms of its fatigue fracture. Transport and Telecommunication 2015;16(2):158-166.
[5] Truman CE, Brooker JD. Analysis of a shrink-fit failure on a gear hub/shaft assrmbly. Eng Fail Anal. 2007;14(4):557-572.
[6] Gujaran S, Gholap S. Fatigue analysis of drive shaft. International Journal of Research in Aeronautical and Mechanical Engineering 2014;2(10):22-28.
[7] Kadam HA, Hyalij NS. Design and analysis of belt conveyor roller shaft. International Journal of Engineering Trends and Technology 2016;36(1).
[8] Deepan Marudachalam MG, Kanthavel K, Krishnaraj R. Optimization of shaft design under fatigue loading using Goodman method. International Journal of Scientific & Engineering Research. 2011;2.8:1-5.
[9] Robert LN. Machine design an integrated approach. Pearson Prentice Hall Publishers, USA. 2006:558-560.
[10] Padhal DK, Meshram DB. Analysis and failure improvement of shaft of gear motor in CRM shop. International Journal of Engineering and Science 2013;3(4):17-24.
[11] Rao SS. The finite element method in engineering. Butterworth-heinemann. 2017.
[12] Maruschak PO, Sorochak AP, Konovalenko IV. Stereoscopic analysis of the stretch zone of a steel specimen cut out of a railway axle and tested for static fracture toughness. Journal of Failure Analysis and Prevention 2015;15(3):436-440.
[13] Crivelli D, Ghelichi R, Guagliano M. Failure analysis of a shaft of a car lift system. Procedia Engineering 2011;10:3683-3691.
[14] Giuseppe P. The finite-element method, Part I. Antennas and Propagation Magazine, IEEE 2007;180-182.
[15] Zerbst U, Maedler K, Hintze H. Fracture mechanics in railway applications – An overview. Fract. Mech. 2005;72:163-194.

[16] Smith RA, Hillmansen S. A brief historical overview of the fatigue of railway axles. Proceedings of the Institution of Mechanical Engineers, Part F: Journal of Rail and Rapid Transit. 2004;218:267-277.
[17] Gravier N, Viet J-J, Leluan A. Predicting the life of railway vehicle axles, Proceedings of the 12th International Wheelset Congress, 1998, Quigdao, China. 1998;133-146.
[18] Zerbst U, Vormvald M, Andersch C, et al. The development of a damage tolerance concept for railway components and its demonstration for a railway axle. Eng. Fract. Mech 2005;72:209-239.
[19] Jian Ping J, Guang M. Investigation on the failure of the gear shaft connected to extruder. Engineering Failure Analysis 2008;15:420-429.
[20] ANSYS, SAS IP, Inc., ANSYS Help System, Mechanical APDL, Theory reference.
[21] Lyashuk OL, Dyachun OL, Badyshchuk VI, Dmytrenko VP. Patent N 109801, Ukraine, B30B 11/00, A23K 40/20 (2016.01) Appliance for the formation of feed briquettes / u201601809, Decl. 25.02.2016, Publ. 12.09.2016, Bull. N17,5.
[22] Lyashuk O, Sokil M, Klendiy V, Skyba O, Dmytrenko V. The study on nonlinear model of dynamics of a system 'extruder elastic auger working body'. Acta Technologica Agriculturae 2016;4:101-106.
[23] Pelaseyed SS, Mashayekhi F, Movahedi-Rad A. Investigation of the shaft failure connected to extruder. Journal of Failure Analysis and Prevention 2015;15:775-781.
[24] Panin SV, Maruschak PO, Vlasov IV, Moiseenko DD, et. al. The role of notch tip shape and radius on deformation mechanisms of 12Cr1MoV steel under impact loading. Part 1. Energy parameters of fracture. Fatigue and Fracture of Engineering Materials and Structures 2016;40:586-596.
[25] Yasniy O, Pyndus Y, Iasnii V, Lapusta Y. Residual lifetime assessment of thermal power plant superheater header. Engineering Failure Analysis 2017;82:390-403.
[26] Stotsko ZA, Sokil BI, Topilnytskyi VG. The impact of structural and kinematic parameters of vibration on the increase of bulk processing intensity. Ukrainian Scientific – Technical Journal. The Vibrations in Engineering and Technology 2002;25:46-52. (in Ukrainian)
[27] Stotsko ZA, Sokil BI, Topilnytskyi VG. Non-linear motion model of a layer of container working environment of vibration machine of bulk processing the products with varying non-linear parameter. Mechanical Engineering 2001;1:19-23.
[28] Sotnykov O, Rodionov M, Maruschak P, Brezinová J, Guzanová A, Apostol Y. Failure analysis of the hinge-lever mould oscillator bearings of the continuous casting machine. Strength, Fracture and Complexity 2014;8(3):135-143.
[29] Subach AP. Forced vibrations of the vibro-impact system in an inelastic collision of the masses. On a problem of dynamics. Riga: Znanie 1996;18:67-78.
[30] Engel B, Al-Maeeni SSH. Failure analysis and fatigue life estimation of a shaft of a rotary draw bending machine. Constraints 2017;3:1785-1790.
[31] Pepper DW, Heinrich JC. The Finite Element Method: Basic Concepts and Applications with MATLAB, MAPLE, and COMSOL. CRC Press. 2017.
[32] Fong JT, Marcal PV, Rainsberger R, Ma L, Heckert NA, Filliben JJ. Finite Element Method Solution Uncertainty, Asymptotic Solution, and a New Approach to Accuracy Assessment. In ASME 2018 Verification and Validation Symposium (pp. V001T12A001-V001T12A001). American Society of Mechanical Engineers 2018.

[33] Nguyen-Xuan H. A polytree-based adaptive polygonal finite element method for topology optimization. International Journal for Numerical Methods in Engineering 2017;110(10):972-1000.
[34] Deepan Marudachalam MG, Kanthavel K, Krishnaraj R. Optimization of shaft design under fatigue loading using Goodman method. International Journal of Scientific & Engineering Research 2011;2(8):1061-1066.
[35] Raut SP, Raut LP. Failure analysis and redesign of shaft of overhead crane. International Journal of Engineering Research and Applications 2014;4(6):130-135.
[36] Popovych PV, Dzyura V, & Shevchuk OS Reliability estimation of transport means elements under the action of cyclic loads and corrosive environment. Int. J. of Automotive and Mechanical Engineering 2018;15(4):5793-5802.